Current Biology 17, 932–939, June 5, 2007 ©2007 Elsevier Ltd All rights reserved DOI 10.1016/j.cub.2007.04.034

Report

ANR5, an FGF Target Gene Product, Regulates Gastrulation in *Xenopus*

Hyeyoung A. Chung,[1] Takamasa S. Yamamoto,[1] and Naoto Ueno[1,2,*]
[1] Division of Morphogenesis
National Institute for Basic Biology
[2] The Graduate University of Advanced Studies
38 Nishigonaka
Myodaiji, Okazaki, 444-8585
Japan

Summary

Gastrulation is a morphogenetic process in which tightly coordinated cell and tissue movements establish the three germ layers (ectoderm, mesoderm, and endoderm) to define the anterior-to-posterior embryonic organization [1]. To elicit this movement, cells modulate membrane protrusions and undergo dynamic cell interactions. Here we report that ankyrin repeats domain protein 5 (xANR5), a novel FGF target gene product, regulates cell-protrusion formation and tissue separation, a process that develops the boundary between the ectoderm and mesoderm [2, 3], during *Xenopus* gastrulation. Loss of xANR5 function by antisense morpholino oligonucleotide (MO) caused a short trunk and spina bifida without affecting mesodermal gene expressions. xANR5-MO also blocked elongation of activin-treated animal caps (ACs) and tissue separation. The dorsal cells of xANR5-MO-injected embryos exhibited markedly reduced membrane protrusions, which could be restored by coinjecting active Rho. Active Rho also rescued the xANR5-MO-inhibited tissue separation. We further demonstrated that xANR5 interacted physically and functionally with paraxial protocadherin (PAPC), which has known functions in cell-sorting behavior, tissue separation, and gastrulation cell movements [4–6], to regulate early morphogenesis. Our findings reveal for the first time that xANR5 acts through Rho to regulate gastrulation and is an important cytoplasmic partner of PAPC, whose cytoplasmic partner was previously unknown.

Results and Discussion

XL023o21, which Encodes Ankyrin Repeats Domain Protein 5, Is a Novel FGF Target

We previously performed a screening with dorsal marginal zone (DMZ) explants treated with the FGF receptor inhibitor SU5402. From this screen, XL023o21 was isolated as a downregulated gene [7]. In the DMZ, the endogenous expression of XL023o21 was suppressed by a dominant-negative FGFR (XFD) or by SU5402 to the background level. Overexpression of eFGF caused the upregulation of XL023o21, which was suppressed by SU5402 treatment. The ectopic expression of eFGF in ACs upregulated XL023o21 expression in a concentration-dependent manner, and this increase was downregulated by SU5402 (Figures 1A and 1B). These data indicate that XL023o21 is an FGF-responsive gene.

XL023o21 encodes ankyrin repeats domain protein 5 (xANR5), which has two predicted functional domains (Figure 1C): both ends contain ankyrin repeats, which act as a scaffold for protein interactions and cytoskeleton binding [8], and the intermediate region contains two EF-hand domains that bind calcium and modulate calcium signaling [9]. BLAST and XDB (http://Xenopus.nibb.ac.jp) searches showed that ANR5 is well conserved across vertebrates, suggesting that it has an evolutionarily important role during development. The *Xenopus* ANR5 and human ANR5 amino acid sequences show 53% identity and 70% similarity overall (Figure 1C). In addition, xANR5 shows 86% identity to its ortholog in *Xenopus tropicalis* (data not shown). xANR5 is maternally expressed during early embryogenesis, and its transcripts are almost ubiquitous but dorsally enriched in the gastrula (Figures S1A and S1B in the Supplemental Data available online). Intriguingly, the expression patterns of PAPC, Fz7, and Rho [5, 10] overlapped with that of xANR5 in the dorsal mesoderm, suggesting that these molecules might function in similar processes.

xANR5-MO Perturbs Early Embryonic Development

To elucidate the function of xANR5 during gastrulation, we performed gain- and loss-of-function analyses. Microinjection of *xANR5* mRNA or xANR5-MO that specifically suppressed the expression of UTR-xANR5-Vns (Figure 1D) caused incomplete blastopore closure (data not shown) and a short trunk and spina bifida (S. B.) at the tadpole stage (Figure 1E). Remarkably, the morphological defects caused by xANR5-MO were rescued by the coinjection of *xANR5*, a rescue construct lacking the MO recognition site, or of *hANR5* mRNA coinjection (Figure 1E). These results indicate that the phenotype was specifically due to xANR5 depletion and that ANR5's function is conserved across phylogeny. Despite the morphological defects, however, embryonic induction and patterning were not disturbed in the *xANR5* mRNA- or xANR5-MO-injected embryos (Figures S2A–S2E).

We further demonstrated that xANR5-MO inhibited the elongation of activin-treated ACs without affecting mesodermal induction (Figure S2E), and this MO-induced inhibition was also efficiently rescued by the overexpression of hANR5 (Figure 1F). These data indicate again that the effect of xANR5-MO was not due to impaired mesodermal formation but rather due to a defect in cell movement. Further evidence for the function of xANR5 in regulating early morphogenetic movements was obtained by analyzing early gastrula that were fixed and sectioned sagittally along the dorsal midline. In the *Xenopus* gastrula, involuted mesodermal cells migrate

*Correspondence: nueno@nibb.ac.jp

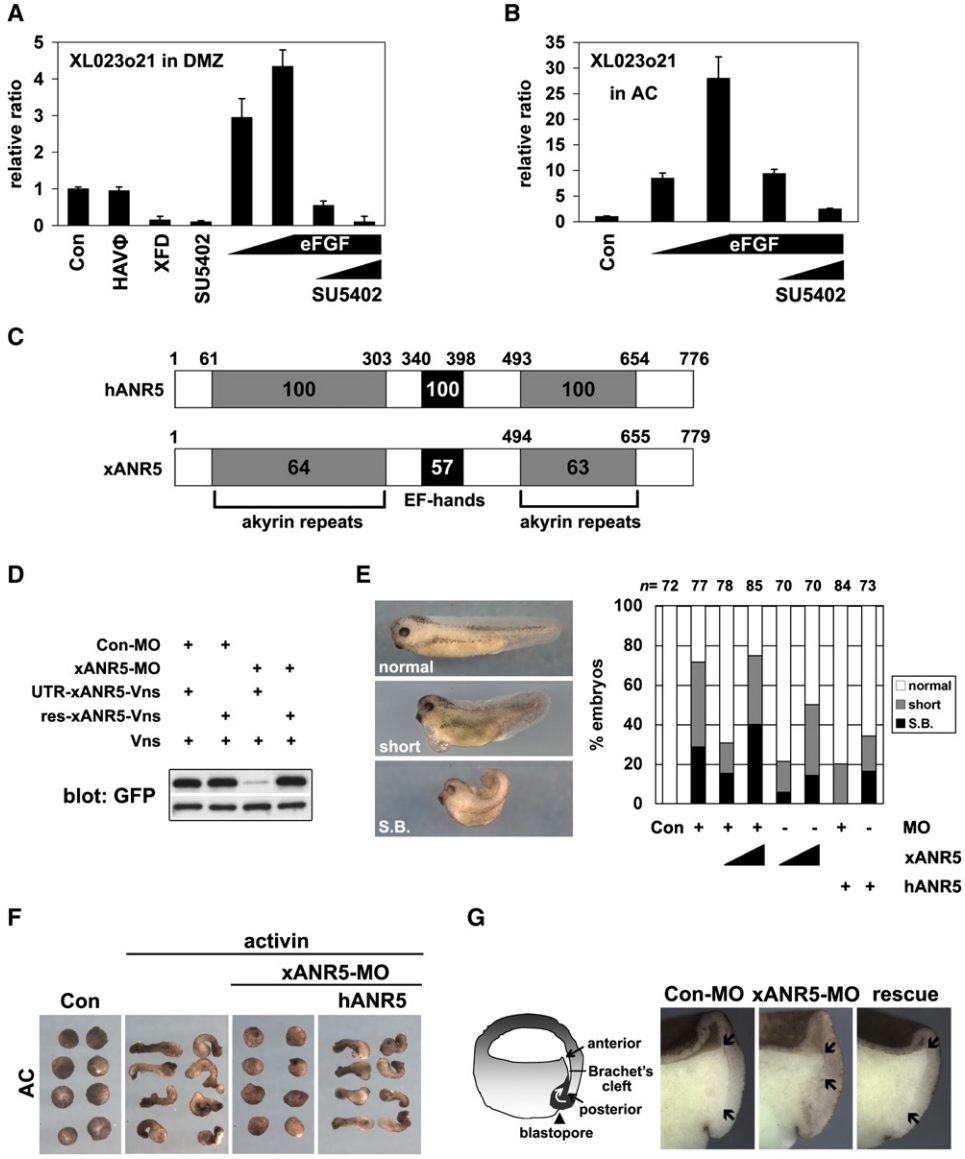

Figure 1. xANR5, an FGF-Responsive Gene Product, Is Important for *Xenopus* Gastrulation

(A and B) XL023o21 was upregulated by the overexpression of eFGF (10, 100 pg) and downregulated by the inhibition of FGF signaling with XFD (500 pg) or SU5402 (25, 50 μM). The results of three experiments are shown. Error bars indicate standard deviation from three different data.

(C) Comparison of the protein structures of human ANR5 (hANR5) and *Xenopus* ANR5 (xANR5). The numbers above and inside the box indicate the amino acid residues and the percent identity between the two proteins, respectively.

(D) The effect of xANR5-MO on the transcription of *xANR5* mRNA was demonstrated with an in vitro transcription/translation system. xANR5-MO specifically inhibited the transcription of the UTR-including *xANR5* mRNA (*UTR-xANR5-Vns*) constructed to generate a fusion protein with eYFP (Vns). The effect of xANR5-MO was restored by coexpression of a rescue construct (*rescue-xANR5-Vns*). xANR5 protein was detected by western blotting with an anti-GFP antibody. Vns protein was detected as a loading control.

(E) Depletion of xANR5 by MO (16.8 ng per embryo) or the overexpression of xANR5 resulted in a short trunk (short) and S.B. These gastrulation-defective phenotypes caused by xANR5-MO were partially restored by the coinjection of *xANR5*, a rescue construct (500 pg), or *hANR5* (400 pg).

(F) When coinjected with activin, xANR5-MO abrogated the activin-induced elongation of animal caps, which was fully rescued by the coinjection of *hANR5*. 20 embryos that had received a microinjection of mRNA or MOs were used for AC isolation at the blastula stage. Ten explants each were used to examine activin-induced elongation and for RT-PCR analysis. The data represent three different experiments.

(G) Schematic diagram of a sagittally fractured early gastrula shows the tissue separation at the DMZ, indicated by the visually identifiable Brachet's cleft. Black arrows indicate the anterior and posterior ends of the cleft, respectively. Embryos fixed at stage 10.5 were fractured through the dorsal blastopore, and the Brachet's cleft formation was analyzed. The Con-MO-injected embryo showed a cleft that extended from the anterior to posterior end, whereas the xANR5-MO-injected embryo showed perturbed posterior cleft formation. Coinjection of a rescue construct restored the extension of the posterior cleft that was inhibited by xANR5-MO microinjection.

away from the blastopore toward the animal pole by crawling on the blastocoel roof (BCR), which consists of noninvoluting ectodermal cells. The development of a morphologically identifiable boundary or cleft (Brachet's cleft) between the mesodermal and ectodermal layer prevents their cells from intermingling [2, 3]. Notably, in the embryos that received an xANR5-MO injection, the boundary between the BCR and the

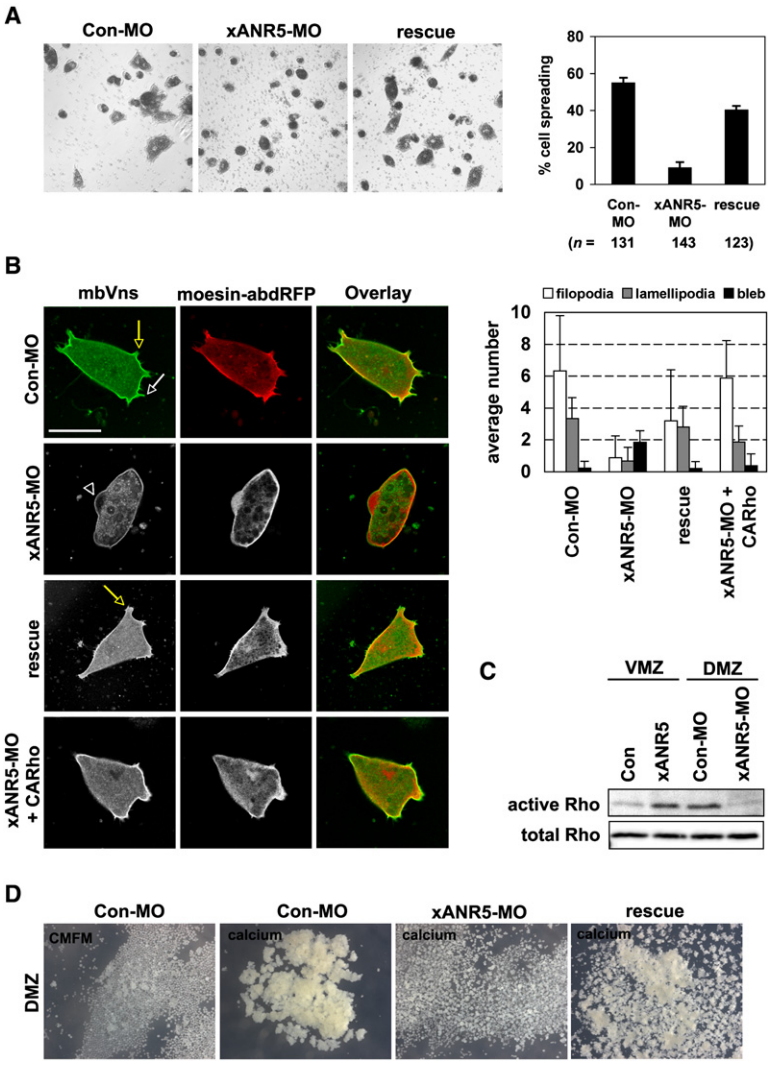

Figure 2. xANR5-MO Abolishes the Cell-Protrusive Morphology

(A and B) The dorsal marginal zone (DMZ) of an embryo that had received a microinjection of MO or mRNA at the 4-cell stage was isolated at stage 10.5 and dissociated in CMFM. Dissociated dorsal cells were plated on a fibronectin-coated glass-bottomed dish, and their spreading on fibronectin was observed after a 1 hr incubation in Steinberg's solution. Unattached cells were removed by gentle washing. Con-MO-injected cells were well spread on the fibronectin and produced fully formed filopodial and lamellipodial protrusions. Membrane blebs were hardly observed in the Con-MO-injected cells. Most of the xANR5-MO-injected cells failed to spread on fibronectin and showed far fewer active protrusions and a higher frequency of membrane blebs than the Con-MO-injected cells. The coinjection of *xANR5* or *CARho* (2.5 pg) could partially and almost completely reverse the effects caused by xANR5-MO, respectively. The white and yellow arrows indicate filopodia and lamellipodia, respectively. Arrowhead indicates a membrane bleb. Error bars indicate standard deviation from three different data. Scale bar represents 50 μm.

(C) The DMZ and ventral marginal zone (VMZ) of embryos that had received a microinjection of MO or mRNA were isolated at stage 10.5 and subjected to a Rho activation assay. Overexpression of xANR5 (1 ng) increased the Rho activity in the VMZ, whereas xANR5-MO downregulated the activation of Rho in the DMZ.

(D) DMZ cell dissociation and reaggregation assay. Cells from DMZs of Con-MO-injected embryos formed a large cell mass upon calcium addition while those from xANR5-MO injected embryos failed to reaggregate, which was rescued by the coinjection of *xANR5*.

involuted mesoderm disappeared posteriorly, and Brachet's cleft was present only anteriorly. This result implies that tissue separation is abrogated by the knocking down of xANR5 expression. The inhibition of the cleft extension caused by xANR5-MO was specific, because the coinjection of a rescue construct (*xANR5*) led to a well-developed posterior cleft (Figure 1G).

Depletion of xANR5 Disrupts Cell Spreading and Cell Protrusion

Gastrulation is a fundamental morphogenetic process regulated by highly orchestrated movements of cells and tissues. For this movement to occur, cells must achieve dynamic modulation of protrusions that are important for the cell motility [1, 11, 12]. We found that DMZ in which xANR5 function had been lost did not show convergent extension (CE) at stage 14, whereas the control-MO (Con-MO)-injected DMZ showed good CE (Figure S3A). Furthermore, at an earlier stage (stage 13), the xANR5-MO-injected dorsal cells failed to become tightly coordinated and were round in shape. These cells produced reduced cell protrusions, such as filopodia and lamellipodia (Figures S3B and S3C). Our data indicate that xANR5 might modulate the cell protrusions. To investigate this possibility more directly, we next examined the morphology at a single-cell level, focusing on the cell protrusions.

Dorsal cells were dissociated from embryos that had received MO or mRNA injection and were incubated for 1 hr on a fibronectin-coated dish, to allow binding. The morphology of the cells that were attached to the fibronectin was then observed. Approximately 60% of the Con-MO-injected cells underwent spreading and flattening. However, the spreading of the xANR5-MO-injected cells was dramatically reduced, with only 10% of the cells showing spreading on fibronectin. The coinjection of a rescue construct restored the cell-spreading effect to the xANR5-MO-injected cells (Figure 2A).

The above results led us to examine the membrane morphology more closely, to determine whether the xANR5-MO modifies the dynamic membrane protrusions like filopodia and lamellipodia, which allow cell-shape change and movements, and the loss of whose function can influence gastrulation [11, 12]. A membrane-bound form of Vns (mbVns) and the actin-binding domain of a moesin-bound form of RFP (moesin-abdRFP)

were coinjected with MO and mRNA. To trace the dynamic movements of the protrusions, we took time-lapse movies of individual cells. Con-MO-injected cells produced dynamic protrusions; the filopodia and lamellipodia were well extended and retracted. In contrast, the xANR5-MO-injected cells showed remarkably fewer and smaller protrusions, which were static and appeared frozen on the fibronectin, and actively generated shape- and location-transforming membrane blebs. The coexpression of the rescue construct with xANR5-MO rescued the effect caused by the loss of xANR5 function and resulted in the production of dynamic membrane protrusions (Figure 2B and Figure S3D).

It is also well known that protrusive cell morphology is regulated by the small GTPase Rho family [12–14]. Thus, we speculated that xANR5 requires the function of small GTPases for its regulation of cell protrusions. Intriguingly, the coexpression of a constitutively active form of Rho (CARho) prevented the reduced protrusions and increased membrane blebs that were induced by the loss of xANR5 function (Figure 2B and Figure S3D). We also found that Rho activity in the DMZ was significantly suppressed by xANR5-MO injection. Overexpression of xANR5 in the VMZ increased the Rho activation (Figure 2C). Taken together, these results clearly indicate that xANR5 regulates cell morphology by modulating Rho activity. In addition, these data are consistent with previous reports showing that the Rho family regulates cell-shape change, adhesion, and migration, which are mediated by the actin cytoskeleton [12–15]. The coinjection of a constitutively active form of *Rac* (*CARac*) did not show a significant rescue effect on the protrusive morphology (data not shown).

xANR5-MO Influences Cell-Cell Adhesion

In our experiments, we noticed that the cells from xANR5-MO-injected embryos were rounded-up and loosely packed in dorsal explants (Figure S3B), suggesting that xANR5 might also control cell-cell adhesion. To test this possibility more directly, we assessed whether xANR5-MO could modulate cell-cell adhesion by using a dissociation and reaggregation assay. DMZs from embryos that had received a microinjection of MO or mRNA were isolated and dissociated in calcium-magnesium-free medium (CMFM) with gentle shaking. We confirmed that the explants were well dissociated in CMFM. Calcium was added, and 2–3 hr later, the cells from the Con-MO-injected embryos had reaggregated and formed a large cell mass, whereas those from the xANR5-MO-injected embryos failed to reaggregate and remained dispersed (Figure 2D). Again, the coexpression of xANR5 rescued the effect of xANR5-MO and resulted in the production of cell clumps. These results support the idea that xANR5 regulates cell-cell adhesion.

xANR5 and PAPC Interact Synergistically in the Formation of Brachet's Cleft

Rho is known as a cytoskeleton regulator. We found that Rho can also rescue the impaired cell morphology caused by xANR5-MO. Recently, Rho was reported to be involved in the development of Brachet's cleft [5]. To examine the role of xANR5 and Rho in tissue separation, xANR5-MO (Figure 1G) and *CARho* were coinjected

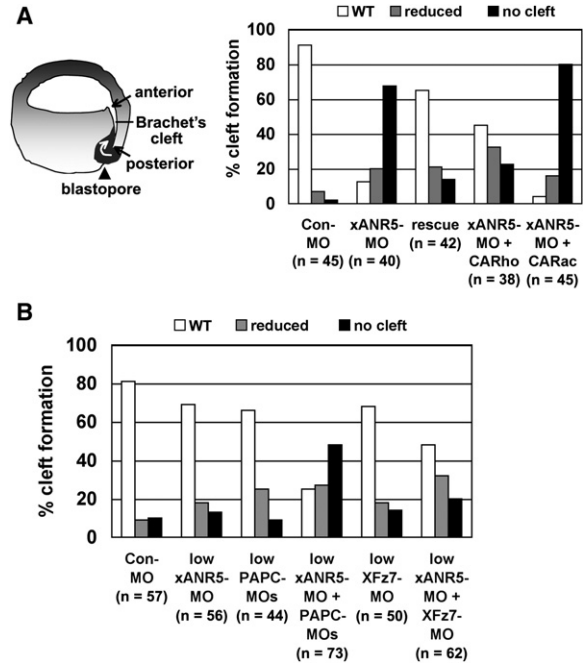

Figure 3. xANR5-MO Inhibits the Development of Brachet's Cleft

Embryos that had received a microinjection of MO or mRNA into the two dorsovegetal blastomeres at the 8-cell stage were fixed at stage 10.5, then sagittally fractured to examine formation of the cleft.

(A) Inhibition of the cleft's extension caused by xANR5-MO was specifically rescued by the coinjection of *xANR5* mRNA. CARho (10 pg) could partially rescue the inhibition of the posterior cleft formation caused by xANR5-MO. However, CARac failed to recover the effect of xANR5-MO on cleft formation.

(B) A low amount of xANR5-MO (4.2 ng), PAPC-MOs (20 ng), and/or Fz7-MO (40 ng) was introduced into dorsovegetal blastomeres by individual injections or coinjection to detect possible interactions among these molecules. Each MO injected alone resulted in a near-normal extension of Brachet's cleft. Coinjection of a low amount of xANR5-MO and PAPC-MOs caused a synergistic inhibition of cleft development and caused a severe defect in the posterior cleft formation, while coinjection of a low amount of xANR5-MO and Fz7-MO showed an additive effect on cleft formation.

into the dorsovegetal side of embryos. Intriguingly, the *CARho*-coinjected embryos showed extension of the posterior cleft, although the effect was partial (Figure 3A). This result supports the idea that xANR5 and Rho, whose activity is regulated by xANR5, interact in tissue separation. The coinjection of *CARac* with xANR5-MO failed to reverse the effect of xANR5-MO; rather, it exacerbated the xANR5-MO effect on the formation of Brachet's cleft. To examine further whether xANR5 influences the separation behavior, we carried out an in vitro tissue-separation assay as described previously [3, 5]. The coinjection of xANR5-MO abolished the separation behavior induced by BVg1 overexpression (Figures S4A–S4C), indicating that xANR5 has a role in the tissue separation.

It was previously demonstrated that XFz7 and PAPC enhance tissue separation, and conversely, that the knockdown of these proteins abolishes the development of Brachet's cleft nonredundantly [3, 5]. We therefore reasoned that xANR5 might interact with XFz7 or PAPC in regulating cleft formation. A low dose of xANR5-MO that was insufficient to inhibit cleft formation

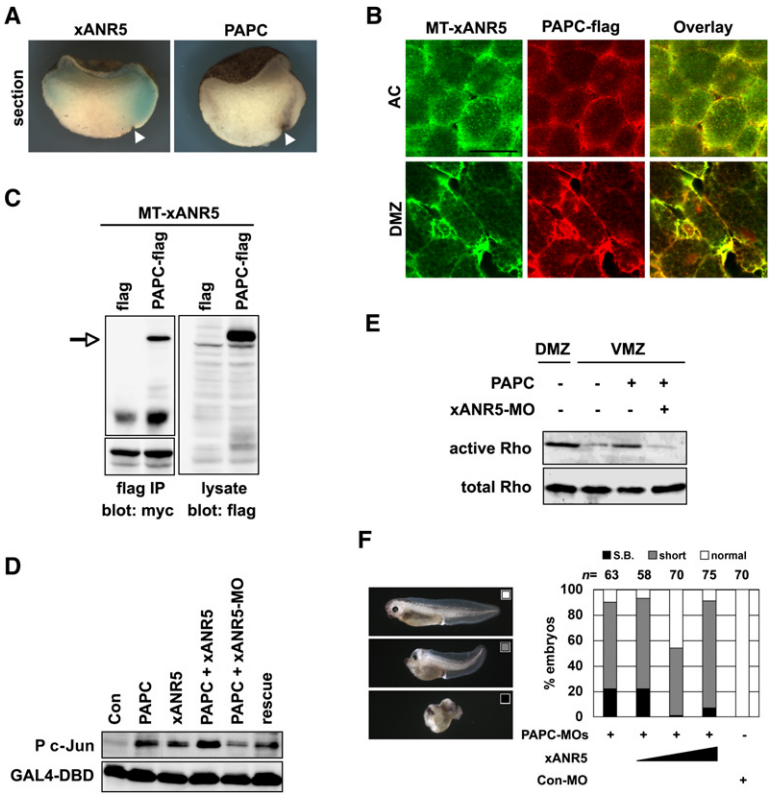

Figure 4. xANR5 Is Physically Associated with PAPC and Indispensable for the PAPC-Dependent Signaling Pathway

(A) Expression patterns of xANR5 and PAPC at the early gastrula were detected with Fluorescein-labeled antisense RNA of xANR5 and DIG-labeled antisense RNA of PAPC. Embryos were fixed at stage 10.5 and sectioned sagittally through the dorsal midline. xANR5 and PAPC were showed overlapping expressions at the DMZ. Arrowheads indicate the blastopore.

(B) Full-length xANR5 was tagged with the 6-repeat myc epitope (MT-xANR5), and full-length PAPC was tagged with the flag epitope (PAPC-flag). *MT-xANR5* (50 pg) and *PAPC-flag* (50 pg) were injected into two animal and dorsal blastomeres at the 2-cell stage and 4-cell stage and then isolated at the blastula and early gastrula stage, respectively. xANR5 was detected with a mouse anti-myc antibody and an Alexa 488-conjugated mouse anti-IgG antibody. PAPC was detected with a rabbit anti-flag antibody and an Alexa 544-conjugated rabbit anti-IgG antibody. Scale bar represents 50 μm.

(C) Immunoprecipitation experiments with MT-xANR5 and PAPC-flag were carried out in 293T culture cells. The expressed proteins were precipitated with a mouse anti-flag antibody (Sigma-Aldrich) and detected with a rabbit anti-flag antibody (Sigma-Aldrich) and mouse anti-myc antibody. A physical interaction between xANR5 and PAPC was determined by western blotting. An arrow indicates PAPC expression detected with a rabbit anti-flag antibody.

(D) A JNK activation assay was carried out with animal blastomeres. The single injection of *PAPC* or *xANR5* enabled the induction of c-*jun* phosphorylation, and the coinjection of *PAPC* and *xANR5* further increased the c-*jun* activity. The phosphorylation of c-*jun* triggered by PAPC overexpression was significantly decreased when xANR5-MO was coinjected, and this effect was rescued by *xANR5* coinjection.

(E) To investigate whether xANR5 is involved in the PAPC-dependent Rho activation, a Rho activation assay was carried out with marginal zone explants. In the VMZ, the overexpression of *PAPC* induced the activation of Rho activity, which was suppressed by the coinjection of xANR5-MO.

(F) The depletion of PAPC by MO injection into the 2 dorsal blastomeres at the 4-cell stage resulted in a short trunk and S.B. Coinjection of *xANR5* mRNA into the dorsal cells could partially rescue the effect of PAPC-MOs.

was coinjected with a low dose of XFz7-MO or PAPC-MOs, followed by a careful analysis of the cleft formation. Surprisingly, when the levels of xANR5 and PAPC were simultaneously lowered by the coinjection of a low amount of each MO, cleft formation was synergistically inhibited; the extension of the posterior cleft was absent in approximately 50% of the embryos, and only about 20% of the embryos showed a wild-type cleft (Figure 3B). However, the coinjection of low doses of xANR5-MO and XFz7-MO showed only an additive effect on the cleft formation, suggesting that xANR5 and XFz7 do not functionally interact. This result was somewhat unexpected, because a previous report showed that the coinjection of low amounts of PAPC-MO and XFz7-MO synergistically inhibited cleft formation, suggesting that these proteins had nonredundant functions. One explanation for the discrepancy is that cytoplasmic complexes or partners of these molecules might modulate or fine-tune each pathway. The tissue separation induced by XFz7 and PAPC requires, respectively, PKC-α activity and Rho activity. However, XFz7-dependent PKC-α activity does not participate in the PAPC-dependent tissue separation [3, 5]. Our findings demonstrating that xANR5-MO and PAPC-MOs, but not xANR5-MO and XFz7-MO, have a synergistic effect on the development of Brachet's cleft imply that xANR5 interacts functionally with PAPC in the regulation of tissue separation. Consequently, we suggest that xANR5 might modulate PAPC function in the regulation of gastrulation.

xANR5 Is Colocalized and Physically Interacted with PAPC

To determine whether xANR5 and PAPC form a complex as binding partners, we first examined the embryonic localization of these two molecules. We performed whole-mount in situ hybridization (WISH) and analyzed the expression patterns of xANR5 and PAPC at the gastrula stage. Embryos fixed at the gastrula stage were fractured sagittally and subjected to the WISH with a Fluorescein-labeled antisense *xANR5* probe (*xANR5-Fluorescein*) and DIG-labeled antisense *PAPC* probe (*PAPC-DIG*) or vice versa. The embryos showed overlapping expression patterns of xANR5 and PAPC in the DMZ (Figure 4A). Next, we examined the subcellular localization of xANR5 and PAPC in ACs and the DMZ with a 6-repeat myc epitope-tagged xANR5 (MT-xANR5) and flag epitope-tagged PAPC (PAPC-flag). The localization of the two epitope-tagged proteins was detected by immunostaining. In ACs, xANR5 (green) was localized to the cytoplasm, apparently near the plasma membrane. In the spindle-shaped dorsal cells, xANR5

accumulated at the mediolateral ends, where the lamellipodial activity orchestrates directional cell movements [11] (Figure 4B). These results were consistent with the localization of xANR5-Vns (Figure S1C). The expression of PAPC (red) was detected near the membrane and at the two tips of bipolarized cells in the AC and DMZ, respectively, as reported previously [6]. In a merged image, the colocalization of xANR5 and PAPC (yellow) was clearly detected near the cell membrane. Notably, in the spindle-shaped dorsal cells, both xANR5 and PAPC were concentrated at the two tips, where they showed overlapping expression (Figure 4B).

To examine the interaction of these two proteins more directly, we performed coimmunoprecipitation and pull-down assays with epitope-tagged proteins. We demonstrated that MT-xANR5 and PAPC-flag interacted in the immunoprecipitation assay (Figure 4C), and we confirmed the physical interaction of xANR5 and PAPC in a GST pull-down assay (Figure S5A). The physical interaction was specific, because we failed to detect any interaction between MT-xANR5 or xANR5-GST and the flag epitope alone. To identify which domain of xANR5 is required for this association, we made several deletion constructs of xANR5 fused with the GST epitope. Among the domains of xANR5, we identified the C-terminal ankyrin repeats domain as the mediator of the physical interaction of xANR5 and PAPC (Figure S5A).

Our findings suggest that PAPC and xANR5 have cooperative roles in gastrulation and further imply that the C-terminal ankyrin repeats domain might be critical in bridging the function of these two proteins. Roles of the cadherin superfamily during embryonic development have been extensively demonstrated [4–6, 16–19]; classical cadherins, which form cytoplasmic complexes with catenins, mediate diverse cell and tissue movements. The protocadherin family is also known to regulate tissue morphogeneses such as tissue separation, gastrulation cell movements, and neural fold formation during embryogenesis. However, unlike classical cadherins, little is known about the cytoplasmic partners or complexes of protocadherin. This is the first report that xANR5, a novel FGF target protein, forms a cytoplasmic complex through its C-terminal ankyrin repeats domain with PAPC, a member of the protocadherin family.

xANR5 Is Indispensable for the PAPC-Regulated Signaling Pathways

The results obtained above led us to speculate further that xANR5 might regulate PAPC-mediated signaling pathways. PAPC was recently proposed to have a signaling function in regulating JNK and Rho [5, 6], which are important molecular components of the PCP pathway [20, 21]. First, we examined whether xANR5 is involved in the regulation of PAPC-dependent JNK activity. The MO and/or mRNA were coinjected with a GAL4-DBD-bound form of c-*jun* into two animal blastomeres at the 2-cell stage. JNK activity was detected by c-Jun phosphorylation. The overexpression of PAPC produced c-Jun phosphorylation, consistent with previous reports [5, 6]. The overexpression of xANR5 also increased the JNK activity. Furthermore, the c-Jun phosphorylation was much more enhanced by the coinjection of xANR5 and PAPC than by a single injection of *xANR5* or *PAPC*. When PAPC and xANR5-MO were simultaneously introduced into the animal blastomeres, interestingly, xANR5-MO inhibited the c-Jun phosphorylation caused by PAPC overexpression, which in turn implies that xANR5-MO abrogated the PAPC-mediated JNK activation. The effect of xANR5-MO on this c-Jun phosphorylation was specific, because the coinjection of *xANR5* could increase the JNK activity in the presence of xANR5-MO (Figure 4D).

Next, we carried out a Rho activation assay and examined whether xANR5-MO, which can also downregulate Rho activity in the DMZ, inhibits PAPC-dependent Rho activation. Microinjection of *PAPC* into the two ventral blastomeres at the 4-cell stage triggered the activation of Rho in the VMZ, where the activity is normally lower than in the DMZ [21, 22]. However, the ectopic Rho activity was reduced when xANR5-MO was coinjected with *PAPC* (Figure 4E). We further examined whether xANR5 could rescue the downregulated Rho activity by PAPC-MO injection in the DMZ. The innate Rho activity in the DMZ was reduced when PAPC-MO was injected into the two dorsal blastomeres at the 4-cell stage. The downregulated Rho activity was completely restored by the coinjection of *xANR5*, suggesting that xANR5 modulates the PAPC-regulated Rho activation (Figure S5B).

The importance of JNK and the Rho family proteins in cell and tissue movements is well conserved across phylogeny [12–14, 20–23]. These proteins are critical elements of the cellular machinery associated with polarized cell motility and cytoskeletal behavior. Recent reports showed that PAPC modulates Rho activation, whose activity regulates not only cell movements but also tissue separation, and our findings were reminiscent of these observations. When xANR5-MO was injected into the dorsal region, we found defects in protrusive cell morphology and gastrulation cell movements. In these DMZs, the Rho activity was remarkably reduced and the formation of Brachet's cleft was inhibited. In addition, the inhibition of the cleft was exacerbated by the coinjection of xANR5-MO and PAPC-MOs. Taken together, the finding that xANR5-MO inhibited PAPC-dependent JNK and Rho activation supports the idea that xANR5 is required for cytoskeletal remodeling and cellular locomotion in PAPC-elicited intracellular responses.

Finally, we performed an embryonic rescue experiment to determine whether xANR5 could compensate for the effect caused by the PAPC-MOs. The microinjection of PAPC-MOs into the two dorsal blastomeres at the 4-cell stage produced phenotypes such as a short trunk and S.B. Interestingly, the coexpression of *xANR5* mRNA restored the phenotypes caused by the PAPC knockdown, although this was a partial effect (Figure 4F). This rescue effect was also confirmed for the Rho activity (Figure S5B). These results clearly indicate that xANR5 plays an important role in the PAPC-dependent signaling pathways that regulate morphogenetic processes.

Conclusions

Our study shows that xANR5, which was identified from a microarray analysis with SU5402-treated DMZs, regulates cell-protrusive morphology and tissue separation

in *Xenopus* gastrulation. Our findings support the idea that xANR5 functions in regulating early morphogenetic movements. The expression of xANR5 is enriched in DMZ and in the two tips of spindle-shaped dorsal cells, where extensive cell and tissue movements occur. xANR5 is colocalized with PAPC, which is known to regulate gastrulation cell movements and tissue separation. xANR5-MO caused defects in the cell-protrusive morphology that is critical for the dynamic cell-shape changes and cell motility by inhibiting Rho activity. In our previous report [12], we demonstrated that NRH, another FGF target gene product, also regulates JNK activity, Rho activity, and protrusive cell morphology. In line with further elucidating the roles of FGF signaling during gastrulation, it would be intriguing to determine whether xANR5 and NRH interact functionally in these events. The knockdown of xANR5 abolished tissue separation and active Rho could rescue the effect of xANR5-MO, suggesting that Rho, an important regulator of the cytoskeleton and cell migration, is required for robust xANR5 activity during gastrulation. We further demonstrated that xANR5 not only physically interacts with PAPC through its C-terminal ankyrin repeats domain, but also functionally interacts in the regulation of JNK and Rho activity. The present work, which identifies a novel functional partner of PAPC in gastrulation regulation, provides further insight into the in vivo role and signaling mechanisms of the protocadherin family, whose cytoplasmic complexes are mostly unknown.

Experimental Procedures

Embryos

Xenopus embryos were obtained by in vitro fertilization and staged according to Nieuwkoop and Faber [24]. For each experiment, the data from at least three different batches of embryos were collected. Embryonic manipulation was carried out as described [12].

Antisense Morpholino Oligonucleotides

The antisense morpholino oligonucleotides (MOs) were obtained from Gene Tools (Philomath, OR). The MO sequences were as follows: xANR5-MO 5′-CTAGTCTTTCTTCTACCTCTGCCAT-3′; PAPC-MOs 5′-CCTAGAAACAGTGTGGCAATGTGAA-3′ and 5′-CTTGCCTAGAAAGAGTGCTGCTGTG-3′; Con-MO 5′-CCTCTTACCTCAGTTACAATTTATA-3′; XFz7-MO 5′-CCAACAAGTGATCTCTGGACAGCAG-3′.

Plasmid Construction and mRNA Preparation for Microinjection

A full-length cDNA clone, XL023o21, was isolated from XDB of the NIBB/NIG *Xenopus* EST database, then inserted in-frame into the EcoRI and XhoI sites of the pCS2+ plasmid by PCR. xANR5, including the 5′UTR, and xANR5 in which silent mutations were introduced (a rescue construct, xANR5) were also inserted into the pCS2+ or pCS2-Venus plasmid. GAL4-DBD-tagged c-*jun* (100 pg injected) was a kind gift from M. Tada. Plasmids to be used for microinjection were linearized with NotI, and capped mRNAs were synthesized as described [12].

RNA Isolation and RT-PCR Analysis

Total RNA was isolated from 10 explants with Trizol reagent (Life Technologies), according to the manufacturer's instructions. Experiments were carried out as previously described [7]. The gel images were scanned and quantified with a FLA2000 Bioimager with built-in software (Fuji Film, Japan).

Cytological Observation by Confocal Microscopy

To observe the subcellular localization of the Venus, RFP, myc, and flag-tagged constructs, we used confocal laser scanning microscopy (Carl Zeiss MicroImaging) with built-in LSM 501 software. ACs isolated at the blastula stage were mounted on a glass-bottomed dish (3910-035; Iwaki). DMZ or VMZ explants were mounted on a glass-bottomed dish coated with fibronectin (~4–10 μg/ml, F1141; Sigma-Aldrich), followed by incubation until the proper stages. Immunostained explants were mounted on a glass slide (Matsunami, JAPAN) or a glass-bottomed dish by Gel/Mount (Biomeda, Foster City, CA). All images were prepared for publication with Adobe Photoshop.

Cell Spreading, Single-Cell Protrusion, and Cell Dissociation and Reaggregation Assay

DMZs isolated at stage 10.5 were dissociated in calcium-magnesium-free medium (CMFM). For the cell-spreading and -protrusion assay, dissociated cells were plated on a fibronectin-coated glass-bottomed dish, then cultured for an hour before observation. The unattached cells were gently washed away. For the cell-spreading assay, the morphology of cells attached to the fibronectin-coated dish was examined by phase-contrast microscopy. We counted the flattened cells that exhibited a multipolar cell shape as spreading cells. To observe the membrane-protrusive morphology, the behaviors of adherent cells were recorded as time-lapse movies. For the dissociation and reaggregation assay, isolated DMZs were gently rocked in CMFM for 1 hr, and then incubated for 3 hr after 4 mM calcium was added to the CMFM.

JNK Assay and Rho Activation Assay

To examine JNK activity, ten ACs from embryos that had received microinjections of GAL4-DBD-tagged c-*jun* (100 pg) with MO and/or mRNA into two animal blastomeres at the 2-cell stage were used. A mouse anti-GAL4-DBD antibody (Santa Cruz) and rabbit anti-phospho c-*jun* antibody (Cell Signaling) were used to detect the total c-*jun* and phosphorylated c-*jun*, respectively. The Rho activation assay was carried out as described [21, 22] by a Rho Activation Assay Biochem Kit (Cytoskeleton, CO).

Protein-Protein Interaction, SDS-PAGE, and Western Blotting

Epitope-fused proteins were harvested from 293T cells, then precipitated with a mouse anti-flag antibody (Sigma-Aldrich) or mouse anti-GST antibody (Santa Cruz). SDS-PAGE and western blotting were carried out as previously described [7, 12]. The antibodies used in the western blotting were as follows: rabbit anti-GFP antibody (Molecular Biological Laboratories), mouse anti-myc antibody, mouse anti-GST antibody (Santa Cruz), mouse anti-flag antibody (Sigma-Aldrich), rabbit anti-flag antibody (Sigma-Aldrich), mouse anti-Rho antibody (Clontech), and rabbit anti-RhoA (119) antibody (Santa Cruz), HRP-conjugated anti-rabbit anti-IgG, and HRP-conjugated anti-mouse anti-IgG (Amersham). The ECL Plus kit (Amersham) was used for detection.

Whole-Mount In Situ Hybridization and Immunohistochemistry

The embryos, explants, DIG (digoxigenin)-labeled RNA probes, Fluorescein-labeled RNA probes, and epitope-tagged synthetic mRNAs to be used for whole-mount in situ hybridization (WISH) and immunostaining were prepared and used as described [12, 25, 26]. For the immunostaining, a mouse anti-myc antibody (Santa Cruz) and a rabbit anti-flag antibody (Sigma-Aldrich) were used as the primary antibodies. Alexa 488-labeled mouse anti-IgG antibody (Molecular Probes) and Alexa 555-labeled rabbit anti-IgG antibody (Molecular Probes) were used to detect the primary antibodies. For the WISH, we used an alkaline phosphatase-conjugated anti-fluorescein antibody (Roche) for Fluorescein-labeled probes and an alkaline phosphotase-conjugated anti-DIG antibody (Roche) for DIG-labeled probes. Embryos were stained with BCIP (Roche) and BCIP+NBT (both from Roche) or BM Purple (Roche) in alkaline phosphatase buffer.

Supplemental Data

Five figures are available at http://www.current-biology.com/cgi/content/full/17/11/932/DC1/.

Acknowledgments

This work was supported by grants from the JSPS to N.U. and from the Ministry of Education, Culture, Sports, Science, and Technology

(MEXT), Japan, to N.U. and to H.A.C. We thank C. Kintner for helpful comments and H. Steinbeisser for communicating unpublished data.

Received: March 9, 2007
Revised: April 11, 2007
Accepted: April 12, 2007
Published online: May 3, 2007

References

1. Keller, R. (2005). Cell migration during gastrulation. Curr. Opin. Cell Biol. *17*, 533–541.
2. Wacker, S., Grimm, K., Joos, T., and Winklbauer, R. (2000). Development and control of tissue separation at gastrulation in *Xenopus*. Dev. Biol. *224*, 428–439.
3. Winklbauer, R., Medina, A., Swain, R.K., and Steinbeisser, H. (2001). Frizzled-7 signaling controls tissue separation during *Xenopus* gastrulation. Nature *413*, 856–860.
4. Kim, S.-H., Yamamoto, A., Bouwmeester, T., Aguis, E., and De Robertis, E.M. (1998). The role of paraxial protocadherin in selective adhesion and cell movements of the mesoderm during *Xenopus* gastrulation. Development *125*, 4681–4690.
5. Medina, A., Swain, R.K., Kuerner, K.-M., and Steinbeisser, H. (2004). *Xenopus* paraxial protocadherin has signaling functions and is involved in tissue separation. EMBO J. *23*, 3249–3258.
6. Unterseher, F., Hefele, J.A., Giehl, K., De Robertis, E.M., Wedlich, D., and Schambony, A. (2004). Paraxial protocadherin coordinates cell polarity during convergent extension via RhoA and JNK. EMBO J. *23*, 3259–3269.
7. Chung, H.A., Hyodo-Miura, J., Terasaka, C., Kitaya, A., Nagamune, T., and Ueno, N. (2004). Screening of FGF target genes in *Xenopus* by microarray analysis: temporal dissection of the signaling pathway using a chemical inhibitor. Genes Cells *9*, 749–761.
8. Mosavi, L.K., Cammett, T.J., Desrosiers, D.C., and Peng, Z.-Y. (2004). The ankyrin repeat as molecular architecture for protein recognition. Protein Sci. *13*, 1435–1448.
9. Lewit-Bentley, A., and Rety, S. (2000). EF-hand calcium-binding proteins. Curr. Opin. Struct. Biol. *10*, 637–643.
10. Wünnenberg-Stapleton, K., Blitz, I.L., Hashimoto, C., and Cho, K.W.Y. (1999). Involvement of the small GTPases XRhoA and XRnd1 in cell adhesion and head formation in early *Xenopus* development. Development *126*, 5339–5351.
11. Wallingford, J.B., Rowning, B.A., Vogeli, K.M., Rothbacher, U., Fraser, S.E., and Harland, R.M. (2000). Dishevelled controls cell polarity during *Xenopus* gastrulation. Nature *405*, 81–85.
12. Chung, H.A., Hyodo-Miura, J., Nagamune, T., and Ueno, N. (2005). FGF signal regulates gastrulation cell movements and morphology through its target NRH. Dev. Biol. *282*, 95–110.
13. Burridge, K., and Wennerberg, K. (2004). Rho and Rac take center stage. Cell *116*, 167–179.
14. Raftopoupou, M., and Hall, A. (2004). Cell migration: Rho GTPases lead the way. Dev. Biol. *265*, 23–32.
15. DeMali, K.A., and Burridge, K. (2003). Coupling membrane protrusions and cell adhesion. J. Cell Sci. *116*, 2389–2397.
16. Heggem, M.A., and Bradley, R.S. (2003). The cytoplasmic domain of *Xenopus* NF-protocadherin interacts with TAF1/set. Dev. Cell *4*, 419–429.
17. Gumbiner, B.M. (2005). Regulation of cadherin-mediated adhesion in morphogenesis. Nat. Rev. Mol. Cell Biol. *6*, 622–634.
18. Halbleib, J.M., and Nelson, W.J. (2006). Cadherins in development: cell adhesion, sorting, and tissue morphogenesis. Genes Dev. *20*, 3199–3214.
19. Chen, X., and Gumbiner, B.M. (2006). Paraxial protocadherin mediates cell sorting and tissue morphogenesis by regulating C-cadherin adhesion activity. J. Cell Biol. *174*, 301–313.
20. Yamanaka, H., Moriguchi, T., Masuyama, N., Kusakabe, M., Hanafusa, H., Takada, R., Takada, S., and Nishida, E. (2002). JNK functions in the non-canonical Wnt pathway to regulate convergent extension movements in vertebrates. EMBO Rep. *3*, 69–75.
21. Habas, R., Kato, Y., and He, X. (2001). Wnt/Frizzled activation of Rho regulates vertebrate gastrulation and requires a novel Formin homology protein Daam1. Cell *107*, 843–854.
22. Habas, R., Dawid, R., and He, X. (2003). Coactivation of Rac and Rho by Wnt/Frizzled signaling is required for vertebrate gastrulation. Genes Dev. *17*, 295–309.
23. Xia, Y., and Karin, M. (2004). The control of cell motility and epithelial morphogenesis by Jun Kinases. Trends Cell Biol. *14*, 94–101.
24. Nieuwkoop, P.D., and Faber, J. (1967). A Normal Table of *Xenopus laevis* (Amsterdam: North Holland Publishing).
25. Harland, R.M. (1991). *In situ* hybridization: an improved whole-mount method for *Xenopus* embryos. Methods Cell Biol. *36*, 685–695.
26. Knecht, A.K., Good, P.J., Dawid, I.G., and Harland, R.M. (1995). Dorsal-ventral patterning and differentiation of noggin-induced neural tissue in the absence of mesoderm. Development *121*, 1927–1935.

Accession Numbers

The GenBank accession number for the full-length cDNA clone XL023o21 reported in this paper is AY553185.